This article has been accepted for publication in a future issue of this journal, but has not been fully edited. Content may change prior to final publication. Citation information: DOI 10.1109/TWC.2017.2777488, IEEE Transactions on Wireless Communications

Leveraging High Order Cumulants for Spectrum Sensing and Power Recognition in Cognitive Radio Networks

Danyang Wang, Ning Zhang, *Member, IEEE*, Zan Li, *Senior Member, IEEE*, Feifei Gao, *Senior Member, IEEE*, and Xuemin (Sherman) Shen, *Fellow, IEEE*

***Abstract*—Hybrid interweave-underlay spectrum access in cognitive radio (CR) networks can explore spectrum opportunities when primary users (PUs) are either active or inactive, which significantly improves spectrum utilization. The practical wireless systems such as Long Term Evolution-Advanced (LTE-A), usually operate at multiple transmission power levels, leading to a multiple primary transmission power (MPTP) scenario. In such a case, the two fundamental issues in hybrid interweave-underlay spectrum access, are to detect the "on/off" status of PUs and to recognize the operating power level of PUs, which are challenging due to non-Gaussian transmitted signals. In this paper, we exploit high order cumulants (HOCs) to efficiently perform spectrum sensing and power recognition. Specifically, for a given order and time lag, we first propose a single HOC based spectrum sensing and power recognition (SCSR) scheme with low computational complexity, by leveraging minimum Bayes risk criterion. Moreover, we propose a hybrid multiple HOCs based spectrum sensing and power recognition (HCSR) scheme with multiple orders and time lags, to further improve the detection performance. Both the proposed schemes can eliminate the adverse impact of the noise power uncertainty. Finally, simulation results are provided to evaluate the proposed schemes.**

***Index Terms*—Cognitive radio, spectrum sensing, high-order cumulants, multiple hypothesis testing, multiple primary transmission power.**

I. Introduction

With proliferation of wireless devices and emergence of diverse wireless services, the available wireless spectrum resource has become severely limited. Meanwhile, conventional fixed spectrum allocation policy suffers from low spectrum utilization. Cognitive radio (CR), first proposed in [1], is deemed as a promising approach to alleviate the insufficiency of spectrum utilization. The fundamental concept for CR networks has been featured as dynamic spectrum access, which allows secondary users (SUs) to opportunistically exploit the spectrum bands that are not heavily occupied by the licensed users [2]–[4].

The dynamic spectrum access strategies are mainly classified into three categories: interweave, underlay, and overlay [5]. The interweave approach is based on the idea of opportunistic communication that SUs exploit the spectrum holes to communicate when the licensed spectrum bands are not used by PU [6]. In the case of underlay paradigm, SUs can always access to the spectrum band if the interference caused to PU is below a given threshold [7]. In overlay systems, the knowledge about the primary network beyond the spectrum occupancy might be obtained at SUs, so that SUs could maintain or further improve the communications of primary network while obtain some additional bandwidth for their own transmissions [8]. Note that these three spectrum access strategies have distinct advantages in improving spectrum utilization. Recently, hybrid schemes that can combine the advantages of different approaches have drawn increasing attentions [9]–[14]. In [9], a hybrid underlay/overlay transmission mode that the access modes are switched based on the activities of PUs, was investigated to improve the network throughput and guarantee the SUs' quality-of-service (QoS) requirements. Then, in [10], an optimal power allocation strategy was proposed for hybrid overlay/underlay spectrum sharing networks, where the SUs join the power auction organized by the relay and bid for maximizing the utility. In [11]–[13], some promising hybrid interweave-underlay spectrum access strategies were studied to utilize the licensed spectrum band more intelligently. In hybrid interweave-underlay spectrum access, the SUs flexibly switch between interweave and underlay schemes according to the spectrum sensing results of the PU's state. If the PU is detected as absent, SUs adopt interweave mode with a higher transmission power to achieve a higher transmission rate. If the PU is detected as present, SUs switch to the underlay mode to transmit with a low power to avoid causing harmful interference to the PU. With hybrid interweave-underlay spectrum access, spectrum utilization can be further improved.

However, almost all these works [6]–[13] only consider PU either being absent or transmitting at a constant power level. In practice, PUs usually operate at different power levels to adapt to the surrounding environments or rate requirements

D. Wang and Z. Li are with the State Key Laboratory of Integrated Service Networks, School of Telecommunications Engineering, Xidian University, Xi'an, 710071, China (e-mail: danyangwang@stu.xidian.edu.cn; zanli@xidian.edu.cn).

N. Zhang is with the Department of Computer Science, Texas A&M University at Corpus Christi, Corpus Christi, TX, 78412, USA (e-mail: ning.zhang@tamucc.edu).

F. Gao is with the Tsinghua National Laboratory for Information Science and Technology, Department of Automation, Tsinghua University, Beijing, 10084, China (e-mail: feifeigao@ieee.org).

X. Shen is with the Department of Electrical and Computer Engineering, University of Waterloo, Waterloo, ON N2L 3G1, Canada (email: xshen@bbcr.uwaterloo.ca).

This work was supported in part by the Key project of National Natural Science Foundation of China under Grant 61631015; by the Fundamental Research Funds for the Central Universities under Grant 7215433803; by the National Natural Science Foundation of China under Grant {61422109, 61531011}; by the Natural Sciences and Engineering Research Councilof Canada (NSERC).

Part of this work was presented at IEEE ICC 2017, Paris, France.

This article has been accepted for publication in a future issue of this journal, but has not been fully edited. Content may change prior to final publication. Citation information: DOI 10.1109/TWC.2017.2777488, IEEE Transactions on Wireless Communications

[15]–[17], as regulated in many standards, e.g., IEEE 802.11 series [18], long-term evalution (LTE) standard [19], and LTE-Advanced standard [20]. When PU can transmit at multiple transmission power levels (i.e., the multiple primary transmission power (MPTP) scenario), PU's interference temperature could vary under different transmission power levels. If SUs switch to the underlay mode to perform transmission with a constant power level, they may cause harmful interference to the PU or waste spectrum opportunities when PU actually operates at a low or high transmission power, respectively. In this scenario, SUs need to know PU's interference temperature by sensing the power level of PU, and then adjust their transmission power to fully exploit spectrum opportunities while preventing PU from being harmfully interfered. Hence, accurately detecting the power level that the PU used should be taken into account when performing spectrum sensing, which is consistent with the original concept of full cognition introduced by Mitola [21].

Spectrum sensing should not only detect the "on/off" status of PU but also recognize the power level when PU has multiple transmission power level. Some preliminary works under MPTP scenarios have been studied. The authors in [22] firstly consider the spectrum sensing and power level recognition in MPTP scenarios, where energy detector is derived as the optimal detector for both detecting the "on/off" status of PU and recognizing the power level of PU under the additive white Gaussian noise (AWGN) conditions. However, it needs to know the accurate noise power, which may not be available to SUs in practice. In our previous work [23], a maximum eigenvalue based sensing and power recognition method for MPTP scenarios is proposed, where multiple antennas are employed to assist SUs to recognize the power level of PU. Note that both [22] and [23] are based on the assumption that the transmitted signals from PU are Gaussian process. While, in many applications [24]–[26], the transmitted signals can be non-Gaussian process such as radar signals, sonar signals, speech, digital modulation signals and etc. For instance, the phase-shift keying (PSK) and M-quadrature amplitude modulation (M-QAM) modulated signals have finite discrete constellations and finite constant amplitude, making the signal distributions far from Gaussian. Therefore, the non-Gaussian signal detection should be taken into account in a realistic CR environment.

To deal with the non-Gaussian input, several spectrum sensing schemes have been proposed [27]–[30]. In [27], the authors investigates frequency domain spectrum sensing methods based on analysis of the discrete Fourier transform of received signals, which allow the PU's signal to be non-Gaussian. In [28], the authors utilize a short-time estimation of third-order cumulant as the test statistic to detect the signal feature. Whereas, only a third-order cumulant of a certain order is used to design the sensing algorithm. Therefore, it fails to exploit the rich statistical information of the received signal. In [29], the authors investigate a detection algorithm of non-Gaussian signals by leveraging the integrated polyspectrum. However, the estimation of integrated polyspectrum is more complicated than that of HOC. In [30], the authors study an optimized high order spectral based detection techniques for non-Gaussian signal, where a F-test statistic is derived. However, the channel state information is not considered, which makes it only an enlightening work for spectrum sensing by using the high order statistics.

In this paper, we investigate spectrum sensing and power recognition in MPTP scenarios considering the non-Gaussian transmitted signals. We propose two spectrum sensing schemes, namely single high-order cumulant based spectrum sensing and power recognition (SCSR) scheme and hybrid multiple high-order cumulants based spectrum sensing and power recognition (HCSR) scheme. For a given order and time lag, the SCSR sensing scheme is proposed based on the minimum Bayes risk criterion. The SCSR sensing scheme has low computational complexity since only the variance of single order cumulant is required to be estimated when calculating the lower bounds and upper bounds of decision regions of all hypotheses. Then, HCSR sensing scheme is proposed with multiple orders and time lags, so that the rich statistical information of the primary signal can be excavated. The HCSR sensing scheme provides more accurate sensing performance at the cost of increasing the computational complexity. Nevertheless, it allows for a compromise between performance and complexity. It is well known that cumulants higher than second order are zero for Gaussian random process. Hence, both the SCSR scheme and HCSR scheme can extract a non-Gaussian signal from Gaussian noise even when the noise is colored. Moreover, the proposed schemes require no information about exact noise power, which makes them robust to noise power uncertainty. For a specific channel realization, closed form expressions of decision regions as well as the closed form sensing performance are derived. Finally, simulation results are provided to validate and evaluate the proposed schemes.

The remainder of this paper is organized as follows: In section II, we formulate the spectrum sensing and power recognition problem of MPTP scenario as well as recall the definitions and estimation of cumulants. Section III presents the spectrum sensing and power recognition scheme based on single high-order cumluant, and provides the performance analysis and some compelling discussions. Moreover, hybrid multiple high-order cumulants based spectrum sensing and power recognition scheme are presented in section IV. Simulation results are provided in Section V, and the conclusions are drawn in Section VI.

II. System Model and Background

A. System Model

Consider a hybrid interweave-underlay spectrum access networks, where PU could either be absent or operate at one of the discrete power levels P_i, $i = 1, 2, \cdots, L$. Without loss of generality, these power levels are arranged as $P_1 < P_2 < \cdots < P_L$. Suppose that once a power level is chosen, it will be used for a certain period, during which SU could perform spectrum sensing and power recognition as well as the subsequent transmission. The n-th received signal samples at SU are given by:

$$\begin{aligned} &\mathcal{H}_0 : x(n) = w(n) \\ &\mathcal{H}_i : x(n) = \sqrt{P_i} h(n) s(n) + w(n), i = 1, \cdots, L \end{aligned} \tag{1}$$

This article has been accepted for publication in a future issue of this journal, but has not been fully edited. Content may change prior to final publication. Citation information: DOI 10.1109/TWC.2017.2777488, IEEE Transactions on Wireless Communications

where $s(n)$ is the non-Gaussian signal transmitted from the PU, $w(n)$ is the additive zero-mean complex colored Gaussian noise, and $h(n)$ represents the flat Rayleigh fading channel from the PU to the SU. In addition, $\mathcal{H}_0$ indicates the PU is absent, and $\mathcal{H}_i$ indicates the PU is operating with transmission power P_i. The flat Rayleigh fading channel $h(n)$ can be represent as $|h|e^{j\phi}$, where $|h|$ and ϕ are the gain and phase elements, respectively. During one sensing period with N samples, the gain and phase of Rayleigh fading channel are assumed constant [31]. In this paper, we aims to derive the detection probability and discrimination probability for a specific channel realization.[1] Moreover, in practical communication systems, the channel information can be obtained at the SU through channel estimation, feedback using the channel reciprocity or the cooperation between the PU and SU.

The noise at the SU may be colored due to oversampling or imperfections in filtering. The colored Gaussian noise $w(n)$ can be regarded as the output of a single pole recursive filter stimulated by a white Gaussian noise (WGN) according to [32, Chap 9]. It can be expressed as $w(n) = -aw(n-1) + u(n)$, where a ($|a| < 1$) is the correlation strength of the noise $w(n)$ and $u(n)$ is WGN with variance σ_u^2. Additionally, the colored Gaussian noise $w(n)$ is assumed to be independent with the PU's signal $s(n)$.

The prior probability of each state of the PU is defined as $\Pr(\mathcal{H}_i), i = 0, 1, \cdots, L$. Define $\mathcal{H}_{\text{on}} = \bigcup_{i=1}^{L} \mathcal{H}_i$ as the hypothesis that the PU is active. Then, the prior probability of $\mathcal{H}_{\text{on}}$ is $\Pr(\mathcal{H}_{\text{on}}) = \sum_{i=1}^{L} \Pr(\mathcal{H}_i)$. In contrast, the inactive state of the PU, denoted by $\mathcal{H}_{\text{off}} \triangleq \mathcal{H}_0$, has the prior probability $\Pr(\mathcal{H}_{\text{off}}) = \Pr(\mathcal{H}_0)$. Assume that the SU has the knowledge of transmission power levels of PU as they are normally predefined and discrete values[2].

B. Estimation of Cumulants

For a random vector $\mathbf{x} = [x_1, x_2, \cdots, x_k]$, the cumulants is defined as the coefficients in the Taylor series expansion of the log of the its characteristic function as follows:

$$\begin{aligned} c_k(\mathbf{x}) &\triangleq cum\{x_1, x_2, \cdots, x_k\} \\ &\triangleq (-j)^k \cdot \left. \frac{\partial^k \ln \Phi(\omega_1, \cdots, \omega_k)}{\partial_{\omega_1} \partial_{\omega_2} \cdots \partial_{\omega_k}} \right|_{\omega_1 = \cdots = \omega_k = 0}, \end{aligned} \tag{2}$$

where $\Phi(\omega_1, \cdots, \omega_k) \triangleq E\{e^{j\omega_1 x_1 + \cdots + j\omega_k x_k}\}$ is the characteristic function of vector $\mathbf{x}$. Based on the definition of cumulants for a random vector, the cumulants for a discrete-time stationary complex process $x(n)$ with lags $\boldsymbol{\tau} = (\tau_1, \cdots, \tau_{k-1})$, is defined by replacing $[x_1, x_2, \cdots, x_k]$ with $[x(n), \cdots, x(n+\tau_{l-1}), x^*(n+\tau_l), \cdots x^*(n+\tau_{k-1})]$

$$\begin{aligned} c_{kx}(\boldsymbol{\tau}) \triangleq cum \Bigg\{ & \underbrace{x(n), \cdots, x(n+\tau_{l-1})}_{l} \\ & \times \underbrace{x^*(n+\tau_l), \cdots, x^*(n+\tau_{k-1})}_{k-l} \Bigg\}, \end{aligned} \tag{3}$$

where $*$ represents the conjugation operation and $0 \le l \le k$. Note that for a given order k, different l will lead to different kth-order cumulants of the complex-valued process. Nevertheless, the following analysis is applicable to each realization of l.

In actual wireless communication applications, usually, finite samplings of the primary signal can be used. According to [33, Chap 2], the kth-order sample cumulant of $x(n), n = 0, \cdots, N-1$ is defined as:

$$\hat{c}_{kx}(\boldsymbol{\tau}) = \sum_{\boldsymbol{v}} (-1)^{(p-1)} (p-1)! \hat{m}_{v_1 x} \cdots \hat{m}_{v_p x}, \tag{4}$$

where $(v_1, \cdots, v_p)$ denotes a partition of $\{1, 2, \cdots, k\}$, p is the size of each partition, and the sum extends over all partitions of the form $v_1, \cdots, v_p$. Additionally, $\hat{m}_{kx}$ is the estimate of the kth-order sample moment of $x(n)$ which can be calculated as

$$\begin{aligned} \hat{m}_{kx}(\boldsymbol{\tau}) = \frac{1}{N} \sum_{n=0}^{N-1} & \underbrace{x(n) \cdots x(n+\tau_{l-1})}_{l} \\ & \times \underbrace{x^*(n+\tau_l) \cdots x^*(n+\tau_{k-1})}_{k-l}. \end{aligned} \tag{5}$$

If $x(n)$ satisfies the following assumption:

Assumption 1.

$$\sum_{\tau_1, \cdots, \tau_{k-1} = -\infty}^{\infty} |\tau_i c_{kx}(\boldsymbol{\tau})| < +\infty, i \in \{1, \cdots, k-1\}. \tag{6}$$

The sample moment $\hat{m}_{kx}(\boldsymbol{\tau})$ is asymptotically unbiased, mean-square sense consistent, i.e., $\lim_{N\to\infty} \hat{m}_{kx}(\boldsymbol{\tau}) = m_{kx}(\boldsymbol{\tau})$. Moreover, $\sqrt{N}\left[\hat{m}_{kx}(\boldsymbol{\tau}) - m_{kx}(\boldsymbol{\tau})\right]$ is asymptotically complex normal [34]. The asymptotic covariance of $\sqrt{N}\hat{m}_{k_1 x}(\boldsymbol{\tau})$ and $\sqrt{N}\hat{m}_{k_2 x}(\boldsymbol{\rho})$ can be expressed as

$$Q_{k_1,k_2}(\boldsymbol{\tau}, \boldsymbol{\rho}) \triangleq \lim_{N\to\infty} N\text{cov}\{\hat{m}_{k_1 x}(\boldsymbol{\tau}), \hat{m}^*_{k_2 x}(\boldsymbol{\rho})\} = S_{2f_{\boldsymbol{\tau},\boldsymbol{\rho}}}(0), \tag{7}$$

where $S_{2f_{\boldsymbol{\tau},\boldsymbol{\rho}}}(\omega) \triangleq \sum_{\xi=-\infty}^{\infty} \text{cov}\{\hat{m}_{k_1 x}(\boldsymbol{\tau}), \hat{m}^*_{k_2 x}(\boldsymbol{\rho})\} e^{-j\omega\xi}$ represents the cross spectrum of $\hat{m}_{k_1 x}(\boldsymbol{\tau})$ and $\hat{m}^*_{k_2 x}(\boldsymbol{\rho})$. In practice, the estimated covariance is used rather than the asymptotic covariance, and the estimate of covariance can be expressed as [35]:

$$\begin{aligned} \hat{Q}_{k_1,k_2}(\boldsymbol{\tau}, \boldsymbol{\rho}) \triangleq & \sum_{\xi} d_s(\xi) \frac{1}{\sum_n d_m(\frac{n}{N})} \sum_n d_m(\frac{n+\xi}{N}) d_m(\frac{n}{N}) \\ & \times [f_{\boldsymbol{\tau}}(n+\xi) - \hat{m}_{f_{\boldsymbol{\tau}}}][f^*_{\boldsymbol{\rho}}(n) - \hat{m}^*_{f_{\boldsymbol{\rho}}}], \end{aligned} \tag{8}$$

[1]To evaluate the performance from a long-term perspective during which the channel gain may vary, an average detection probability and discrimination probability can be calculated by taking average over the probability density function of channel gain. While, in this paper, we focus on deriving the detection probability and discrimination probability for a specific channel realization.

[2]Or, the user's behavior can be obtained alternatively by statistically learning from a long run.

This article has been accepted for publication in a future issue of this journal, but has not been fully edited. Content may change prior to final publication. Citation information: DOI 10.1109/TWC.2017.2777488, IEEE Transactions on Wireless Communications

where $d_s(\xi)$ is a symmetric real valued spectral window with $d_s(0)=1$, $d_m(n)$ is a tapering window of bounder variations that vanishes for $|n|>1$, and $f_{\boldsymbol{\tau}}(n)$ and $\hat{m}_{f_{\boldsymbol{\tau}}}$ are defined as:

$$f_{\boldsymbol{\tau}}(n) \triangleq x(n)x(n+\tau_1)\cdots x(n+\tau_{k-1}), \tag{9}$$

$$\hat{m}_{f_{\boldsymbol{\tau}}} \triangleq \frac{\sum\limits_n d_m(\frac{n}{N}) f_{\boldsymbol{\tau}}(n)}{\sum\limits_n d_m(\frac{n}{N})}. \tag{10}$$

According to [34], $\hat{c}_{kx}(\boldsymbol{\tau})$ is also asymptotically unbiased, mean-square sense consistent, and $\sqrt{N}\left[\hat{c}_{kx}(\boldsymbol{\tau})-c_{kx}(\boldsymbol{\tau})\right]$ is asymptotically complex normal, if $x(n)$ satisfies *Assumption* 1. The estimated covariance between $\sqrt{N}\hat{c}_{k_1x}(\boldsymbol{\tau})$ and $\sqrt{N}\hat{c}_{k_2x}(\boldsymbol{\rho})$ can be calculated using (8) as

$$\hat{T}_{k_1,k_2}(\boldsymbol{\tau},\boldsymbol{\rho}) = \sum_{\mu}\sum_{v}(-1)^{p+q-2}(p-1)!\times(q-1)! \times \sum_{l_1=1}^{p}\sum_{l_2=1}^{q}\prod_{\substack{m_1=1\\ m_1\neq l_1}}^{p}\hat{m}_{\mu_{m_1x}}\prod_{\substack{m_2=1\\ m_2\neq l_2}}^{q}\hat{m}_{\mu_{m_2x}}\hat{Q}_{l_1,l_2}(\boldsymbol{\tau}_{l_1},\boldsymbol{\tau}_{l_2}). \tag{11}$$

III. Spectrum Sensing and Power Recognition Based on Single HOC

In this section, we propose a spectrum sensing and power recognition algorithm based on single high-order cumulant for non-Gaussian inputs in colored Gaussian noise scenario. Based on N received samples in one sensing period, the estimate of $c_{kx}(\boldsymbol{\tau})$ are

$$\begin{aligned}\mathcal{H}_0 &: \hat{c}_{kx}(\boldsymbol{\tau}) = c_{kw}(\boldsymbol{\tau}) + \varepsilon_{kx}^{(N)}(\boldsymbol{\tau}),\\ \mathcal{H}_i &: \hat{c}_{kx}(\boldsymbol{\tau}) = P_i^{k/2}|h|^k e^{j\phi(2l-k)}c_{ks}(\boldsymbol{\tau}) + c_{kw}(\boldsymbol{\tau}) + \varepsilon_{kx}^{(N)}(\boldsymbol{\tau}),\end{aligned} \tag{12}$$

where $\varepsilon_{kx}^{(N)}(\boldsymbol{\tau})$ denotes the estimation error that will be vanished asymptotically as $N\to\infty$. If $w(n)$ is a Gaussian random process, its cumulants higher than second order are zero whereas that of a non-Gaussian random process are not. When $x(n)$ is zero-mean (if not, one can estimate and subtract the mean), given a certain k and lag $\boldsymbol{\tau}$ with $\boldsymbol{\tau}=[\tau_1,\cdots,\tau_{k-1}]$, we assume $c_{ks}(\boldsymbol{\tau})$ exist while $c_{kw}(\boldsymbol{\tau})$ vanish. Hence, Eq. (12) can be expressed as

$$\begin{aligned}\mathcal{H}_0 &: \hat{c}_{kx}(\boldsymbol{\tau}) = \varepsilon_{kx}^{(N)}(\boldsymbol{\tau}),\\ \mathcal{H}_i &: \hat{c}_{kx}(\boldsymbol{\tau}) = P_i^{k/2}|h|^k e^{j\phi(2l-k)}c_{ks}(\boldsymbol{\tau}) + \varepsilon_{kx}^{(N)}(\boldsymbol{\tau}).\end{aligned} \tag{13}$$

As mentioned above, $\sqrt{N}\left[\hat{c}_{kx}(\boldsymbol{\tau})-c_{kx}(\boldsymbol{\tau})\right]$ is asymptotically normal, and the estimated variance σ_c^2 of $\hat{c}_{kx}(\boldsymbol{\tau})$ can be calculated as $\sigma_c^2 = 1/N\cdot\hat{T}_{k,k}(\boldsymbol{\tau},\boldsymbol{\tau})$ by using (11). To simplify the notation, let us denote $|h|^k e^{j\phi(2l-k)}c_{ks}(\boldsymbol{\tau})$ as $c_{ks,h}(\boldsymbol{\tau})$. Moreover, define $P_0=0$ as the equivalent transmission power level when PU is absent. Then, the PDF of $\hat{c}_{kx}(\boldsymbol{\tau})$ under hypothesis $\mathcal{H}_i$ can be expressed as

$$\hat{c}_{kx}(\boldsymbol{\tau}) \sim \mathcal{CN}(P_i^{k/2}c_{ks,h}(\boldsymbol{\tau}), \sigma_c^2). \tag{14}$$

In MPTP scenarios, the primary target is to detect the presence or the absence of PU signal, while the secondary target is to recognize the power-level of PU transmitter. Hence, it is necessary to first verify the hypothesis $\mathcal{H}_{\rm on}/\mathcal{H}_{\rm off}$ and then to recognize which $\mathcal{H}_i, i\geq 1$ is true when $\mathcal{H}_{\rm on}$ is detected.

A. Detection of PU's Presence

The ratio of the posterior probabilities between two hypothesis can be written as

$$\begin{aligned}\xi(\hat{c}_{kx}(\boldsymbol{\tau})) &= \frac{\Pr(\mathcal{H}_{\rm on}|\hat{c}_{kx}(\boldsymbol{\tau}))}{\Pr(\mathcal{H}_{\rm off}|\hat{c}_{kx}(\boldsymbol{\tau}))} = \frac{\sum\limits_{i=1}^{L}\Pr(\mathcal{H}_i)p(\hat{c}_{kx}(\boldsymbol{\tau})|\mathcal{H}_i)}{\Pr(\mathcal{H}_0)p(\hat{c}_{kx}(\boldsymbol{\tau})|\mathcal{H}_0)}\\ &= \sum_{i=1}^{L}\frac{\Pr(\mathcal{H}_i)}{\Pr(\mathcal{H}_0)}\exp\left\{\begin{array}{c}\frac{P_i^{k/2}\{c_{ks,h}^*(\boldsymbol{\tau})\hat{c}_{kx}(\boldsymbol{\tau})+c_{ks,h}(\boldsymbol{\tau})\hat{c}_{kx}^*(\boldsymbol{\tau})\}}{\sigma_c^2}\\ -\frac{P_i^k|h|^{2k}|c_{ks}(\boldsymbol{\tau})|^2}{\sigma_c^2}\end{array}\right\}\\ &= \sum_{i=1}^{L}\frac{\Pr(\mathcal{H}_i)}{\Pr(\mathcal{H}_0)}\exp\left\{\begin{array}{c}\frac{2P_i^{k/2}\times{\rm Re}\{c_{ks,h}^*(\boldsymbol{\tau})\cdot\hat{c}_{kx}(\boldsymbol{\tau})\}}{\sigma_c^2}\\ -\frac{P_i^k|h|^{2k}|c_{ks}(\boldsymbol{\tau})|^2}{\sigma_c^2}\end{array}\right\}.\end{aligned} \tag{15}$$

It can be seen that $\xi(\hat{c}_{kx}(\boldsymbol{\tau}))$ is strictly increasing over ${\rm Re}\{c_{ks,h}^*(\boldsymbol{\tau})\cdot\hat{c}_{kx}(\boldsymbol{\tau})\}$, and the decision rule can be made as follows:

$$T_{\rm SCSR} = {\rm Re}\{c_{ks,h}^*(\boldsymbol{\tau})\cdot\hat{c}_{kx}(\boldsymbol{\tau})\} \underset{\mathcal{H}_{\rm off}}{\overset{\mathcal{H}_{\rm on}}{\gtrless}} \theta, \tag{16}$$

where θ is the pre-determined parameter. It is obvious that, $T_{\rm SCSR}$ obeys Gaussian distribution under the hypothesis $\mathcal{H}_i, i\in 0,1,\cdots,L$, i.e.,

$$\mathcal{H}_i : T_{\rm SCSR} \sim \mathcal{N}(P_i^{k/2}|h|^{2k}|c_{ks}(\boldsymbol{\tau})|^2, |h|^{2k}|c_{ks}(\boldsymbol{\tau})|^2\sigma_c^2). \tag{17}$$

The false alarm probability $\Pr_{\rm fa}$ and the detection probability $\Pr_{\rm d}$ can be calculated as below, respectively,

$$\begin{aligned}\Pr_{\rm fa}(\theta) &= \Pr(\mathcal{H}_{\rm on}|\mathcal{H}_{\rm off}) = \Pr(T_{\rm SCSR}>\theta|\mathcal{H}_{\rm off})\\ &= Q\left(\frac{\theta}{|h|^k|c_{ks}(\boldsymbol{\tau})|\cdot\sigma_c}\right),\\ \Pr_{\rm d}(\theta) &= \Pr(\mathcal{H}_{\rm on}|\mathcal{H}_{\rm on}) = \Pr(T_{\rm SCSR}>\theta|\mathcal{H}_{\rm on})\\ &= \sum_{i=1}^{L}\frac{\Pr(\mathcal{H}_i)}{\Pr(\mathcal{H}_{\rm on})}Q\left(\frac{\theta-P_i^{k/2}|h|^{2k}|c_{ks}(\boldsymbol{\tau})|^2}{|h|^k|c_{ks}(\boldsymbol{\tau})|\cdot\sigma_c}\right),\end{aligned} \tag{18}$$

where $Q(\cdot)$ is the Complementary Cumulative Distribution Function (CCDF), i.e., the right tail probability of the standard normal distribution.

Denote $\theta_{\rm on/off}^{(\cdot)}$ as the decision threshold for detecting the "on/off" status of PU. The superscript indicates which criterion is used, e.g., "NP" indicates Neyman-Pearson criterion is used while "MAP" indicates maximum a posterior probability criterion is adopted. When the objective is to maximize the detection probability $\Pr_{\rm d}$ while keeping the false alarm probability $\Pr_{\rm fa}$ under certain ε_1, NP criterion should be used. Then, we can the calculate the threshold $\theta_{\rm on/off}^{\rm NP}$ for the "on/off" status of PU as

$$\theta_{\rm on/off}^{\rm NP} = |h|^k|c_{ks}(\boldsymbol{\tau})|\sigma_c\cdot Q^{-1}(\varepsilon_1), \tag{19}$$

where $Q^{-1}(\cdot)$ is the inverse function of $Q(\cdot)$. Then the detection probability $\Pr_{\rm d}$ can be calculated as

$$\Pr_{\rm d} = \sum_{i=1}^{L}\frac{\Pr(\mathcal{H}_i)}{\Pr(\mathcal{H}_{\rm on})}Q\left(Q^{-1}(\varepsilon_1) - \frac{P_i^{k/2}|h|^k|c_{ks}(\boldsymbol{\tau})|}{\sigma_c}\right). \tag{20}$$

When the objective is to minimize the *probability of error* $\Pr_{\rm e} = \Pr(\mathcal{H}_{\rm on}|\mathcal{H}_{\rm off})\Pr(\mathcal{H}_{\rm off}) + \Pr(\mathcal{H}_{\rm off}|\mathcal{H}_{\rm on})\Pr(\mathcal{H}_{\rm on})$, the

This article has been accepted for publication in a future issue of this journal, but has not been fully edited. Content may change prior to final publication. Citation information: DOI 10.1109/TWC.2017.2777488, IEEE Transactions on Wireless Communications

MAP detection criterion should be applied. In such case, we compare the ratio $\xi(\hat{c}_{kx}(\boldsymbol{\tau}))$ in (15) with the value 1, which can be formulated as

$$\xi(\hat{c}_{kx}(\boldsymbol{\tau})) = \frac{\Pr(\mathcal{H}_{\rm on}|\hat{c}_{kx}(\boldsymbol{\tau}))}{\Pr(\mathcal{H}_{\rm off}|\hat{c}_{kx}(\boldsymbol{\tau}))} \underset{\mathcal{H}_{\rm off}}{\overset{\mathcal{H}_{\rm on}}{\gtrless}} 1. \tag{21}$$

Taking a deformation of (21), we have

$$\Delta = \sum_{i=1}^{L} \Pr(\mathcal{H}_i) \exp\left\{\frac{2P_i^{k/2} T_{\rm SCSR} - P_i^k |h|^{2k} |c_{ks}(\boldsymbol{\tau})|^2}{\sigma_c^2}\right\} - \Pr(\mathcal{H}_0) \underset{\mathcal{H}_{\rm off}}{\overset{\mathcal{H}_{\rm on}}{\gtrless}} 0. \tag{22}$$

The threshold $\theta_{\rm on/off}^{\rm MAP}$ for detecting the presence or the absence of the PU can be calculated by setting $\Delta = 0$. As Δ is strictly increasing with $T_{\rm SCSR}$, Δ has at least one value below 0 as long as $\Pr(\mathcal{H}_0)$ is large enough. Hence, there exists one and only one threshold $\theta_{\rm on/off}^{\rm MAP}$ that can satisfy

$$T_{\rm SCSR} \underset{\mathcal{H}_{\rm off}}{\overset{\mathcal{H}_{\rm on}}{\gtrless}} \theta_{\rm on/off}^{\rm MAP}. \tag{23}$$

The threshold $\theta_{\rm on/off}^{\rm MAP}$ in MAP criterion can be calculated numerically for detecting whether the PU is present or not. Thus, the detection probability $\Pr_{\rm d}$ in MAP criterion can be obtained by substituting $\theta_{\rm on/off}^{\rm MAP}$ into Eq. (18).

Remark 1. We introduce two ways to obtain the threshold for detecting "on/off" status of the PU, which can be chosen on the user's demands. In the following, we choose MAP criterion but the results can be easily extended to the case with NP criterion.

B. Recognition of PU's Transmission Power Level

When the PU is detected as present, the next step is to recognize at which power level the PU transmitter is operating. Since the PU has more than one transmission power levels, the SU might make various errors in this process. In order to distinguish the PU's transmission power level, which is formulated as multiple hypothesis testing problem, the Bayes risk is employed. Define K_{ij} as the cost when the SU claims the PU operates on power level P_i while the PU is actually transmitting on power level P_j and denote this situation as $\mathcal{H}_i|\mathcal{H}_j$. Then, the expected cost or Bayes risk becomes

$$\mathcal{R} = \sum_{i=1}^{L}\sum_{j=1}^{L} K_{ij} \Pr(\mathcal{H}_i|\mathcal{H}_j;\hat{\mathcal{H}}_{\rm on}) \Pr(\mathcal{H}_j;\hat{\mathcal{H}}_{\rm on}), \tag{24}$$

where $\hat{\mathcal{H}}_{\rm on}$ denotes that the SU has detected the presence of the PU.

Theorem 1. *The Bayes risk $\mathcal{R}$ is minimized if the following decision rule is made.*

$$i^* = \arg\min_i \mathcal{K}_i(\hat{c}_{kx}(\boldsymbol{\tau})), \tag{25}$$

where $\mathcal{K}_i(\hat{c}_{kx}(\boldsymbol{\tau})) = \sum_{j=1}^{L} K_{ij} Pr(\mathcal{H}_j|\hat{c}_{kx}(\boldsymbol{\tau}))$. *Particularly, when the values of cost K_{ij} are assigned as*

$$K_{ij} = \begin{cases} 0, & i = j; \\ 1, & i \neq j, \end{cases} \tag{26}$$

then the decision rule turns into MAP criterion shown as follow, where $\mathcal{H}_0$ is not included in.

$$i^* = \arg\max_i Pr(\mathcal{H}_i|\hat{c}_{kx}(\boldsymbol{\tau}); \hat{\mathcal{H}}_{\rm on}). \tag{27}$$

Proof: See Appendix A. ∎

Using Bayes rule, the posterior probability of hypothesis $\mathcal{H}_i$ can be written as

$$\begin{aligned}\Pr(\mathcal{H}_i|\hat{c}_{kx}(\boldsymbol{\tau}); \hat{\mathcal{H}}_{\rm on}) &= \frac{p(\hat{c}_{kx}(\boldsymbol{\tau})|\mathcal{H}_i; \hat{\mathcal{H}}_{\rm on}) \Pr(\mathcal{H}_i|\hat{\mathcal{H}}_{\rm on})}{p(\hat{c}_{kx}(\boldsymbol{\tau})|\hat{\mathcal{H}}_{\rm on})} \\ &= \frac{p(\hat{c}_{kx}(\boldsymbol{\tau})|\mathcal{H}_i) \Pr(\mathcal{H}_i)}{p(\hat{c}_{kx}(\boldsymbol{\tau})|\hat{\mathcal{H}}_{\rm on}) \Pr(\hat{\mathcal{H}}_{\rm on})}.\end{aligned} \tag{28}$$

We define the equivalent region of $\hat{c}_{kx}(\boldsymbol{\tau})$ for $\{T_{\rm SCSR} > \theta_{\rm on/off}^{\rm MAP}\}$ as $\{\hat{c}_{kx}(\boldsymbol{\tau}) \in R_{\rm on}\}$. Then, the MAP criterion can be rewritten as

$$i^* = \arg\max_i p(\hat{c}_{kx}(\boldsymbol{\tau})|\mathcal{H}_i) \Pr(\mathcal{H}_i),\ \hat{c}_{kx}(\boldsymbol{\tau}) \in R_{\rm on}, \tag{29}$$

where $R_{\rm on}$ represents the region where the PU has been detected as present. For a hypothesis pair $(\mathcal{H}_i, \mathcal{H}_j), \forall i, j \geq 1$, $\mathcal{H}_i$ is determined rather than $\mathcal{H}_j$ if

$$p(\hat{c}_{kx}(\boldsymbol{\tau})|\mathcal{H}_i) \Pr(\mathcal{H}_i) > p(\hat{c}_{kx}(\boldsymbol{\tau})|\mathcal{H}_j) \Pr(\mathcal{H}_j),\ \hat{c}_{kx}(\boldsymbol{\tau}) \in R_{\rm on}. \tag{30}$$

Remark 2. When using MAP criterion for detecting the PU's transmission power level, it is independent with how $\hat{\mathcal{H}}_{\rm on}$ is made. Hence, we can apply either MAP criterion or NP criterion in checking whether the PU is present or not in step one without affecting Eq. (30).

With Eq. (14), we can expand Eq. (30) as

$$\frac{\Pr(\mathcal{H}_i)}{\Pr(\mathcal{H}_j)} \exp\left\{\begin{array}{c} \frac{2(P_i^{k/2} - P_j^{k/2}) T_{\rm SCSR}}{\sigma_c^2} \\ -\frac{(P_i^k - P_j^k)|h|^{2k}|c_{ks}(\boldsymbol{\tau})|^2}{\sigma_c^2} \end{array}\right\} > 1. \tag{31}$$

Then, we calculate the decision region $\mathcal{D}(\mathcal{H}_i)$ of hypothesis $\mathcal{H}_i$ from Eq. (31) by converting it into

$$\begin{aligned}(P_i^{k/2} - P_j^{k/2}) T_{\rm SCSR} > {} & \frac{\sigma_c^2}{2} \ln\left[\frac{\Pr(\mathcal{H}_j)}{\Pr(\mathcal{H}_i)}\right] \\ & + \frac{(P_i^k - P_j^k)|h|^{2k}|c_{ks}(\boldsymbol{\tau})|^2}{2}.\end{aligned} \tag{32}$$

Define

$$\Theta(i,j) \triangleq \frac{\frac{\sigma_c^2}{2} \ln\left[\frac{\Pr(\mathcal{H}_j)}{\Pr(\mathcal{H}_i)}\right] + \frac{(P_i^k - P_j^k)|h|^{2k}|c_{ks}(\boldsymbol{\tau})|^2}{2}}{P_i^{k/2} - P_j^{k/2}}. \tag{33}$$

If $i > j$, i.e., $P_i > P_j$, we can derive

$$T_{\rm SCSR} > \Theta(i,j),\ \forall i > j; \tag{34}$$

If $i < j$, i.e., $P_i < P_j$, then we have

$$T_{\rm SCSR} < \Theta(i,j),\ \forall i < j. \tag{35}$$

For $1 < i < L$, the lower bound of $\mathcal{D}(\mathcal{H}_i)$ should be $\max_{1 \leq j < i} \Theta(i,j)$ and the upper bound of $\mathcal{D}(\mathcal{H}_i)$ should be $\min_{i < j \leq L} \Theta(i,j)$. Moreover, the MAP detection is defined on the domain $\hat{c}_{kx}(\boldsymbol{\tau}) \in R_{\rm on}$, i.e., $T_{\rm SCSR} > \theta_{\rm on/off}^{\rm MAP}$, and hence all decision regions of non-zero power levels should stay in

This article has been accepted for publication in a future issue of this journal, but has not been fully edited. Content may change prior to final publication. Citation information: DOI 10.1109/TWC.2017.2777488, IEEE Transactions on Wireless Communications

$(\theta_{\text{on/off}}^{\text{MAP}}, +\infty)$. In summary, the decision regions of hypotheses $\mathcal{H}_i$'s, $i \in \{1, 2, \cdots, L\}$ can be expressed as (36) shown at the bottom of this page.

For hypothesis $\mathcal{H}_0$, the decision region is $(-\infty, \theta_{\text{on/off}}^{\text{MAP}}]$. Define $\theta_i,\ i \in \{1, 2, \cdots, L\}$ as the threshold between $\mathcal{D}(\mathcal{H}_{i-1})$ and $\mathcal{D}(\mathcal{H}_i)$. Obviously, there is $\theta_1 \triangleq \theta_{\text{on/off}}^{\text{MAP}}$. Moreover, we define $\theta_0 \triangleq -\infty$, and $\theta_{L+1} \triangleq +\infty$ for consistence and completeness. Note that the establishment of the lower bound and upper bound of $\mathcal{H}_i$'s is not related to the noise power, hence the proposed SCSR method is robust to noise uncertainty.

Remark 3. Compared with the traditional spectrum sensing scheme that has only one threshold, multiple thresholds are required in the MPTP scenario, to distinguish the different transmission power levels, as shown in Fig. 1. If the test statistics is no larger than θ_1, the SU declares that the PU is absent, i.e., the channel is idle. When the test statistics falls into the decision region $(\theta_i,\ \theta_{i+1}]$, the SU claims that the PU is working on transmission power P_i.

There exists an interesting phenomenon in MPTP scenarios where some primary power levels could not be detected. Namely, for a certain decision region $\mathcal{D}(\mathcal{H}_{i_0})$, its lower bound may be greater than the upper bound, i.e.,

$$\max\{\theta_{\text{on/off}}^{\text{MAP}}, \max_{1\le j<i_0} \Theta(i_0, j)\} > \min_{i_0<j\le L} \Theta(i_0, j). \tag{37}$$

Once this phenomenon happens, the decision region $\mathcal{D}(\mathcal{H}_{i_0})$ is empty and the power level P_{i_0} can never be detected. We name this phenomenon as *power mask* effect. There are many reasons giving rise to the *power mask* effect, and we give two main reasons as follows:

- If the transmission power level P_{i_0} is seldom used by the PU, i.e., the priori probability of $\Pr(\mathcal{H}_{i_0})$ is very small, then the power level P_{i_0} may be easily ignored by the SU.
- If P_{i_0} is very close to the adjacent power level P_{i_0-1} and P_{i_0+1}, then P_{i_0} is very likely to be masked by P_{i_0-1} or P_{i_0+1} whenever the instantaneous noise influence is large.

Remark 4. When a special case that $\Pr(\mathcal{H}_i) = \Pr(\mathcal{H}_j),\ \forall i, j \in \{1, 2, \cdots, L\}$ is considered in MPTP scenarios, we have

$$\Theta(i, j) = \Theta(j, i) = \frac{(P_i^{k/2} + P_j^{k/2})|h|^{2k}|c_{ks}(\boldsymbol{\tau})|^2}{2}, \tag{38}$$

which is strictly increasing with P_j for any P_i. Then, we have

$$\max_{1\le j<i} \Theta(i, j) = \Theta(i, i-1) < \Theta(i, i+1) = \min_{i<j\le L} \Theta(i, j). \tag{39}$$

Hence, in this special case, the non-zero power levels cannot mask each other, and the *power mask* effect may only happen when P_0 masks the non-zero power levels.

Fig. 2 shows an example to illustrate the *power mask* effect. There are three non-zero power levels (i.e., P_1, P_2, P_3), and the corresponding priori probabilities $\Pr(P_i), i = 1, 2, 3$ are set as 0.1, 0.3, 0.2, respectively. Therefore, the priori probability $\Pr(P_0)$ is 0.4. The decision thresholds and decision regions for each hypothesis $\mathcal{H}_i, i = 0, 1, 2, 3$ are demonstrated in the figure. For hypothesis $\mathcal{H}_1$, its lower bound $\theta_{\text{on/off}}^{\text{MAP}}$ is calculated by Eq. (22), and shown in Fig. 2 as the intersection of the hypothesis $\mathcal{H}_0$ and $\mathcal{H}_{\text{on}}$. Its upper bound is derived as $\Theta(1, 2)$, and is shown as the intersection of the hypothesis $\mathcal{H}_1$ and $\mathcal{H}_2$. It can be seen that the lower bound of decision region $\mathcal{D}(\mathcal{H}_1)$ is greater than its upper bound, and hence the transmission power P_1 cannot be detected due to the *power mask* effect. When P_1 is masked, we set the threshold $\theta_2 = \theta_1$, so the decision region $\mathcal{D}(\mathcal{H}_1)$ is empty.

Different with the traditional binary hypothesis detection, it is not adequate to only evaluate the detection probability $\Pr_{\text{d}}$ in MPTP scenarios. Therefore, we define $\Pr(\mathcal{H}_i|\mathcal{H}_j)$ as the probability that SU claims PU operating at power level P_i while PU actually operates at P_j. Then, we have

$$\begin{aligned}\Pr(\mathcal{H}_i|\mathcal{H}_j) =& \int_{\theta_i}^{\theta_{i+1}} p(T_{\text{SCSR}}|\mathcal{H}_j) dT_{\text{SCSR}} \\ =& Q\left(\frac{\theta_i - P_j^{k/2}|h|^{2k}|c_{ks}(\boldsymbol{\tau})|^2}{|h|^k|c_{ks}(\boldsymbol{\tau})|\sigma_c}\right) \\ & - Q\left(\frac{\theta_{i+1} - P_j^{k/2}|h|^{2k}|c_{ks}(\boldsymbol{\tau})|^2}{|h|^k|c_{ks}(\boldsymbol{\tau})|\sigma_c}\right).\end{aligned} \tag{40}$$

Additionally, for the MPTP scenario, we introduce a new probability to describe the discrimination capability of SU, which should be defined as

$$\Pr_{\text{dis1}} = \frac{1}{\Pr(\mathcal{H}_{\text{on}})} \sum_{i=1}^{L} \Pr(\mathcal{H}_i)\Pr(\mathcal{H}_i|\mathcal{H}_i). \tag{41}$$

Remark 5. $\Pr_{\text{fa}}$ and $\Pr_{\text{d}}$ can also be calculated using the metric $\Pr(\mathcal{H}_i|\mathcal{H}_j)$:

$$\Pr_{\text{fa}} = \Pr(\mathcal{H}_{\text{on}}|\mathcal{H}_{\text{off}}) = \sum_{i=1}^{L} \Pr(\mathcal{H}_i|\mathcal{H}_0); \tag{42}$$

$$\Pr_{\text{d}} = \Pr(\mathcal{H}_{\text{on}}|\mathcal{H}_{\text{on}}) = \frac{1}{\Pr(\mathcal{H}_{\text{on}})} \sum_{i=1}^{L}\sum_{j=1}^{L} \Pr(\mathcal{H}_j|\mathcal{H}_i)\Pr(\mathcal{H}_i). \tag{43}$$

For the computational complexity of SCSR scheme, it comes from two parts: computation of sample cumulant $\hat{c}_{kx}\boldsymbol{\tau}$

$$\mathcal{D}(\mathcal{H}_i) = \begin{cases} T_{\text{SCSR}} \in (\theta_{\text{on/off}}^{\text{MAP}}, \min\limits_{1<j\le L} \Theta(1, j)] & , i = 1; \\ T_{\text{SCSR}} \in (\max\{\theta_{\text{on/off}}^{\text{MAP}}, \max\limits_{1\le j<i} \Theta(i, j)\}, \min\limits_{i<j\le L} \Theta(i, j)] & , 1 < i < L; \\ T_{\text{SCSR}} \in (\max\{\theta_{\text{on/off}}^{\text{MAP}}, \max\limits_{1\le j<L} \Theta(L, j)\}, +\infty) & , i = L. \end{cases} \tag{36}$$

This article has been accepted for publication in a future issue of this journal, but has not been fully edited. Content may change prior to final publication. Citation information: DOI 10.1109/TWC.2017.2777488, IEEE Transactions on Wireless Communications

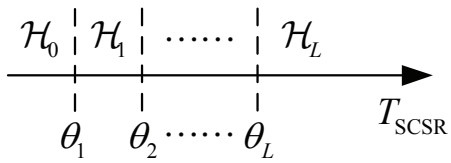

Fig. 1. Multiple thresholds for multiple hypothesis detection.

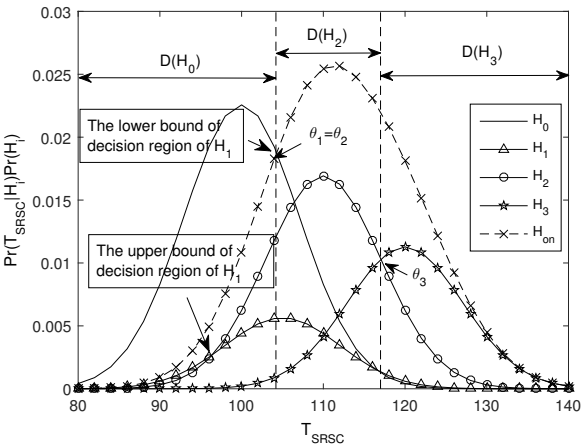

Fig. 2. Illustration for power mask effect in MPTP scenarios.

and computation of the covariance of the sample cumulant. For the first part, $V(k-1)N$ multiplications and $\sum_{i=1}^{V} p_i(N-1)$ additions are needed, where V is the number of the partitions of $\{1,2,\cdots,k\}$, and p_i is the number of the parts in each partition. For the second part, $\sum_{i=1}^{V}\sum_{j=1}^{V}\sum_{l_1=1}^{p_i}\sum_{l_2=1}^{q_j}[(\sum_{\substack{m_1=1\\m_1\neq l_1}}^{p_i}\mu_{m_1}+\sum_{\substack{m_2=1\\m_2\neq l_2}}^{q_j}\mu_{m_2})N+(\mu_{l_1}+\mu_{l_2})T^2+3T]$ multiplications and $\sum_{i=1}^{V}\sum_{j=1}^{V}\sum_{l_1=1}^{p_i}\sum_{l_2=1}^{q_j}((p_i+q_j-2)(N-1)+T(T+4))$ additions are needed, where μ_i is the size of ith partition of $\{1,2,\cdots,k\}$, and T is the window length of $d_s(\xi)$. Note that the computational complexity of SCSR scheme mainly depends on the second part. While in the special but realistic case where $\Pr(\mathcal{H}_i)=\Pr(\mathcal{H}_j)$, the covariance of $\hat{c}_{kx}(\boldsymbol{\tau})$ is no longer needed when pre-calculating the lower bound and upper bound of each hypothesis. Hence, the proposed SCSR scheme has very low computational complexity in this case.

IV. Spectrum Sensing and Power Recognition Based on Multiple HOCs

In this section, we examine the hybrid multiple high-order cumulants based spectrum sensing and power recognition (HCSR) scheme where multiple orders and lags are used. We choose multiple different orders and time lags to make use of the rich statistical information contained in the primary signal so that the HCSR scheme is superior and more flexible. Compared with the SCSR scheme, HCSR method achieves a more reliable sensing and power recognition performance although it may increase the computational complexity. Nevertheless, HCSR method allows us to make a compromise between performance and complexity. Given $\{k_1,\cdots,k_M\}$ and M lag vectors $\{\boldsymbol{\tau}_1,\cdots,\boldsymbol{\tau}_M\}$ with $\boldsymbol{\tau}_i=[\tau_1,\cdots,\tau_{k_i-1}]$, we define a $1\times M$ vector $\mathcal{C}_{kx}(\boldsymbol{T})\triangleq[c_{k_1x}(\boldsymbol{\tau}_1),\cdots,c_{k_Mx}(\boldsymbol{\tau}_M)]$ and its estimate $\hat{\mathcal{C}}_{kx}(\boldsymbol{T})$ can be written as

$$\hat{\mathcal{C}}_{kx}(\boldsymbol{T})\triangleq[\hat{c}_{k_1x}(\boldsymbol{\tau}_1),\cdots,\hat{c}_{k_Mx}(\boldsymbol{\tau}_M)]. \tag{44}$$

When using multiple different orders and different lags, Eq. (13) yields

$$\begin{aligned}\mathcal{H}_0&:\hat{\mathcal{C}}_{kx}(\boldsymbol{T})=\mathcal{E}_{kx}^{(N)}(\boldsymbol{T}),\\ \mathcal{H}_i&:\hat{\mathcal{C}}_{kx}(\boldsymbol{T})=P_i^{k/2}\mathcal{C}_{ks}(\boldsymbol{T})+\mathcal{E}_{kx}^{(N)}(\boldsymbol{T}),\end{aligned} \tag{45}$$

where $\mathcal{C}_{ks}(\boldsymbol{T})$ and $\mathcal{E}_{kx}^{(N)}(\boldsymbol{T})$ are respectively defined as

$$\begin{aligned}\mathcal{C}_{ks}(\boldsymbol{T})&=[c_{k_1s,h}(\boldsymbol{\tau}_1),\cdots,c_{k_Ms,h}(\boldsymbol{\tau}_M)],\\ \mathcal{E}_{kx}^{(N)}(\boldsymbol{T})&=[\varepsilon_{k_1x}^{(N)}(\boldsymbol{\tau}_1),\cdots,\varepsilon_{k_Mx}^{(N)}(\boldsymbol{\tau}_M)],\end{aligned}$$

and $c_{k_is,h}(\boldsymbol{\tau}_i)$ is denoted by $|h|^{k_i}e^{j\phi(2l_i-k_i)}c_{k_is}(\boldsymbol{\tau}_1)$. Notice that, $\sqrt{N}[\hat{\mathcal{C}}_{kx}-\mathcal{C}_{kx}]=\sqrt{N}[\hat{\mathcal{C}}_{kx}-P_i^{k/2}\mathcal{C}_{ks}]$ [3] is asymptotically normal since $\sqrt{N}\,[\hat{c}_{kx}(\boldsymbol{\tau})-c_{kx}(\boldsymbol{\tau})]$ is asymptotically normal, and the (m,n)th entry of the covariance matrix Σ of $\hat{\mathcal{C}}_{kx}$ can be calculated by using Eq. (11). Then, the PDF of $\hat{\mathcal{C}}_{kx}$ can be expressed as

$$\begin{aligned}p(\hat{\mathcal{C}}_{kx}|\mathcal{H}_i)&=\frac{1}{\pi^M|\Sigma|}\\ &\times\exp\left\{-\left(\hat{\mathcal{C}}_{kx}-P_i^{k/2}\mathcal{C}_{ks}\right)\Sigma^{-1}\left(\hat{\mathcal{C}}_{kx}-P_i^{k/2}\mathcal{C}_{ks}\right)^H\right\}.\end{aligned} \tag{46}$$

A. Detection of the PU's Presence

To find the status whether PU is active on its licensed spectrum or not, it is necessary to check the following ratio

$$\begin{aligned}\psi(\hat{\mathcal{C}}_{kx})&=\frac{\Pr(\mathcal{H}_{\text{on}}|\hat{\mathcal{C}}_{kx})}{\Pr(\mathcal{H}_{\text{off}}|\hat{\mathcal{C}}_{kx})}=\frac{\sum_{i=1}^{L}\Pr(\mathcal{H}_i)p(\hat{\mathcal{C}}_{kx}|\mathcal{H}_i)}{\Pr(\mathcal{H}_0)p(\hat{\mathcal{C}}_{kx}|\mathcal{H}_0)}\\ &=\sum_{i=1}^{L}\frac{\Pr(\mathcal{H}_i)}{\Pr(\mathcal{H}_0)}\exp\left\{\begin{array}{c}P_i^{\frac{k}{2}}(\hat{\mathcal{C}}_{kx}\Sigma^{-1}\mathcal{C}_{ks}^H+\mathcal{C}_{ks}\Sigma^{-1}\hat{\mathcal{C}}_{kx}^H)\\ -P_i^k\mathcal{C}_{ks}\Sigma^{-1}\mathcal{C}_{ks}^H\end{array}\right\}.\end{aligned} \tag{47}$$

Since $\psi(\hat{\mathcal{C}}_{kx})$ is increasing with $\hat{\mathcal{C}}_{kx}\Sigma^{-1}\mathcal{C}_{ks}^H+\mathcal{C}_{ks}\Sigma^{-1}\hat{\mathcal{C}}_{kx}^H$, the decision rule can be

$$T_{\text{HCSR}}=\hat{\mathcal{C}}_{kx}\Sigma^{-1}\mathcal{C}_{ks}^H+\mathcal{C}_{ks}\Sigma^{-1}\hat{\mathcal{C}}_{kx}^H\underset{\mathcal{H}_{\text{off}}}{\overset{\mathcal{H}_{\text{on}}}{\gtrless}}\gamma, \tag{48}$$

where γ is the pre-determined threshold. Note that the test statistic derived here is different from single HOC based sensing and recognition algorithm. Nevertheless, T_{HCSR} also obeys Gaussian distribution under the hypothesis $\mathcal{H}_i, i\in 0,1,\cdots,L$, i.e.,

$$\mathcal{H}_i: T_{\text{HCSR}}\sim\mathcal{N}(2P_i^{k/2}\mathcal{C}_{ks}\Sigma^{-1}\mathcal{C}_{ks}^H, 4\mathcal{C}_{ks}\Sigma^{-1}\mathcal{C}_{ks}^H). \tag{49}$$

[3]For easy expression, $\hat{\mathcal{C}}_{kx}$, $\mathcal{C}_{kx}$ and $\mathcal{C}_{ks}$ are used to respectively indicate $\hat{\mathcal{C}}_{kx}(\boldsymbol{T})$, $\mathcal{C}_{kx}(\boldsymbol{T})$ and $\mathcal{C}_{ks}(\boldsymbol{T})$ ignoring the delay parameter vector $\boldsymbol{T}$.

This article has been accepted for publication in a future issue of this journal, but has not been fully edited. Content may change prior to final publication. Citation information: DOI 10.1109/TWC.2017.2777488, IEEE Transactions on Wireless Communications

With Eq. (48) and Eq. (49), the false alarm probability and detection probability can be derived as

$$\mathrm{Pr}_{\mathrm{fa}}(\gamma)=\mathrm{Pr}(\mathcal{H}_{\mathrm{on}}|\mathcal{H}_{\mathrm{off}})=Q\left(\frac{\gamma}{2\sqrt{\mathcal{C}_{ks}\Sigma^{-1}\mathcal{C}_{ks}^{H}}}\right), \tag{50}$$

$$\begin{aligned}\mathrm{Pr}_{\mathrm{d}}(\gamma)&=\mathrm{Pr}(\mathcal{H}_{\mathrm{on}}|\mathcal{H}_{\mathrm{on}})\\&=\sum_{i=1}^{L}\frac{\mathrm{Pr}(\mathcal{H}_i)}{\mathrm{Pr}(\mathcal{H}_{\mathrm{on}})}Q\left(\frac{\gamma-2P_i^{k/2}\mathcal{C}_{ks}\Sigma^{-1}\mathcal{C}_{ks}^{H}}{2\sqrt{\mathcal{C}_{ks}\Sigma^{-1}\mathcal{C}_{ks}^{H}}}\right).\end{aligned} \tag{51}$$

If NP criterion is used, we control the false alarm probability $\mathrm{Pr}_{\mathrm{fa}}$ under certain ε_2, and hence the threshold $\gamma_{\mathrm{on/off}}^{\mathrm{NP}}$ can be calculated as

$$\gamma_{\mathrm{on/off}}^{\mathrm{NP}}=2\sqrt{\mathcal{C}_{ks}\Sigma^{-1}\mathcal{C}_{ks}^{H}}Q^{-1}(\varepsilon_2). \tag{52}$$

Then, the detection probability of HCSR method is derived as

$$\mathrm{Pr}_{\mathrm{d}}=\sum_{i=1}^{L}\frac{\mathrm{Pr}(\mathcal{H}_i)}{\mathrm{Pr}(\mathcal{H}_{\mathrm{on}})}Q\left(Q^{-1}(\varepsilon_2)-P_i^{k/2}\sqrt{\mathcal{C}_{ks}\Sigma^{-1}\mathcal{C}_{ks}^{H}}\right). \tag{53}$$

If MAP criterion is used, we will compare the ratio $\psi(\hat{\mathcal{C}}_{kx})$ with the value 1, which can be shown as

$$\psi(\hat{\mathcal{C}}_{kx})=\frac{\mathrm{Pr}(\mathcal{H}_{\mathrm{on}}|\hat{\mathcal{C}}_{kx})}{\mathrm{Pr}(\mathcal{H}_{\mathrm{off}}|\hat{\mathcal{C}}_{kx})}\underset{\mathcal{H}_{\mathrm{off}}}{\overset{\mathcal{H}_{\mathrm{on}}}{\gtrless}}1. \tag{54}$$

With Eq. (49), we can rewrite Eq. (54) as follows:

$$\begin{aligned}\Phi=\sum_{i=1}^{L}\mathrm{Pr}(\mathcal{H}_i)\exp\left\{P_i^{k/2}T_{\mathrm{HCSR}}-P_i^{k}\mathcal{C}_{ks}\Sigma^{-1}\mathcal{C}_{ks}^{H}\right\}\\-\mathrm{Pr}(\mathcal{H}_0)\underset{\mathcal{H}_{\mathrm{off}}}{\overset{\mathcal{H}_{\mathrm{on}}}{\gtrless}}0.\end{aligned} \tag{55}$$

The threshold $\gamma_{\mathrm{on/off}}^{\mathrm{MAP}}$ can be calculated by setting $\Phi=0$. As Φ is strictly increasing with T_{HCSR}, Φ has at least one value below 0 as long as $\mathrm{Pr}(\mathcal{H}_{\mathrm{off}})$ is large enough. Similar to the derivation of $\theta_{\mathrm{on/off}}^{\mathrm{MAP}}$, the threshold $\gamma_{\mathrm{on/off}}^{\mathrm{MAP}}$ can be also calculated numerically.

B. Recognition of PU's Transmission Power Level

After PU is detected, power recognition is performed. As verified in section III-B, from MAP criterion, the optimal decision is "i" if

$$p(\hat{\mathcal{C}}_{kx}|\mathcal{H}_i)\mathrm{Pr}(\mathcal{H}_i)>p(\hat{\mathcal{C}}_{kx}|\mathcal{H}_j)\mathrm{Pr}(\mathcal{H}_j),\ \hat{\mathcal{C}}_{kx}\in R_{\mathrm{on}} \tag{56}$$

Substituting (46) into (56), we have

$$\begin{aligned}(P_i^{k/2}-P_j^{k/2})T_{\mathrm{HCSR}}>&\ln\left[\frac{\mathrm{Pr}(\mathcal{H}_j)}{\mathrm{Pr}(\mathcal{H}_i)}\right]\\&+(P_i^{k}-P_j^{k})\mathcal{C}_{ks}\Sigma^{-1}\mathcal{C}_{ks}^{H}.\end{aligned} \tag{57}$$

Define

$$\Xi(i,j)\triangleq\frac{\ln\left[\frac{\mathrm{Pr}(\mathcal{H}_j)}{\mathrm{Pr}(\mathcal{H}_i)}\right]+(P_i^{k}-P_j^{k})\mathcal{C}_{ks}\Sigma^{-1}\mathcal{C}_{ks}^{H}}{P_i^{k/2}-P_j^{k/2}}. \tag{58}$$

As $P_1<P_2<\cdots<P_L$, then for $j=1,\cdots,i-1,P_i>P_j$, while for $j=i+1,\cdots,L,P_i<P_j$. According to Eq. (57), we can derive

$$\max_{1\le j<i}\Xi(i,j)<T_{\mathrm{HCSR}}<\min_{i<j\le L}\Xi(i,j). \tag{59}$$

Hence, the decision regions of hypothesis $\mathcal{H}_i,\ i\in\{1,2,\cdots,L\}$ can be calculated as (60) shown at the bottom of this page. For hypothesis $\mathcal{H}_0$, the decision region is $(-\infty,\gamma_{\mathrm{on/off}}^{\mathrm{MAP}}]$. Define $\gamma_i,\ i\in\{1,2,\cdots,L\}$ as the threshold between $\mathcal{R}(\mathcal{H}_{i-1})$ and $\mathcal{R}(\mathcal{H}_i)$. Then, we have $\gamma_1\triangleq\gamma_{\mathrm{on/off}}^{\mathrm{MAP}}$. Moreover, we define $\gamma_0\triangleq-\infty,\gamma_{L+1}\triangleq+\infty$ for consistence and completeness. We can note that the noise power is not required when establishing the lower bound and upper bound of $\mathcal{H}_i$'s, hence HCSR method is robust to the noise uncertainty.

The *power mask* effect still exists when hybrid multiple HOCs are used to design the sensing algorithm, although the hybrid multiple HOCs based sensing and power recognition algorithm can make use of the rich statistical information of the received signal. When $\mathrm{Pr}(\mathcal{H}_i)=\mathrm{Pr}(\mathcal{H}_j),\ \forall i,j\in\{1,2,\cdots,L\}$ is considered in MPTP scenarios, we have

$$\Xi(i,j)=\Xi(j,i)=(P_i^{k/2}+P_j^{k/2})\mathcal{C}_{ks}\Sigma^{-1}\mathcal{C}_{ks}^{H}, \tag{61}$$

which is strictly increasing with P_j for any P_i. Then, we have

$$\max_{1\le j<i}\Xi(i,j)=\Xi(i,i-1)<\Xi(i,i+1)=\min_{i<j\le L}\Xi(i,j). \tag{62}$$

Hence, the non-zero power levels cannot mask each other, and the *power mask* effect may only happen when P_0 masks the non-zero power levels.

To evaluate the performance, we first calculate the decision probability $\mathrm{Pr}(\mathcal{H}_i|\mathcal{H}_j)$, as follows:

$$\begin{aligned}\mathrm{Pr}(\mathcal{H}_i|\mathcal{H}_j)=&\int_{\gamma_i}^{\gamma_{i+1}}p(T_{\mathrm{HCSR}}|\mathcal{H}_j)dT_{\mathrm{HCSR}}\\=&Q\left(\frac{\gamma_i-2P_j^{k/2}\mathcal{C}_{ks}\Sigma^{-1}\mathcal{C}_{ks}^{H}}{2\sqrt{\mathcal{C}_{ks}\Sigma^{-1}\mathcal{C}_{ks}^{H}}}\right)\\&-Q\left(\frac{\gamma_{i+1}-2P_j^{k/2}\mathcal{C}_{ks}\Sigma^{-1}\mathcal{C}_{ks}^{H}}{2\sqrt{\mathcal{C}_{ks}\Sigma^{-1}\mathcal{C}_{ks}^{H}}}\right).\end{aligned} \tag{63}$$

According to (41), (42) and (51), the recognition probability, false alarm probability and detection probability of hybrid multiple HOCs based sensing and power recognition algorithm can be calculated using the metric $\mathrm{Pr}(\mathcal{H}_i|\mathcal{H}_j)$, given in (63).

$$\mathcal{R}(\mathcal{H}_i)=\begin{cases}T_{\mathrm{HCSR}}\in(\gamma_{\mathrm{on/off}}^{\mathrm{MAP}},\min\limits_{1<j\le L}\Xi(1,j)] & ,i=1;\\ T_{\mathrm{HCSR}}\in(\max\{\gamma_{\mathrm{on/off}}^{\mathrm{MAP}},\max\limits_{1\le j<i}\Xi(i,j)\},\min\limits_{i<j\le L}\Xi(i,j)] & ,1<i<L;\\ T_{\mathrm{HCSR}}\in(\max\{\gamma_{\mathrm{on/off}}^{\mathrm{MAP}},\max\limits_{1\le j<L}\Xi(L,j)\},+\infty) & ,i=L.\end{cases} \tag{60}$$

This article has been accepted for publication in a future issue of this journal, but has not been fully edited. Content may change prior to final publication. Citation information: DOI 10.1109/TWC.2017.2777488, IEEE Transactions on Wireless Communications

Considering the computational complexity of the HCSR scheme, $\sum_{i=1}^{M} V_i(k_i - 1)N$ multiplications and $\sum_{i=1}^{M}\sum_{j=1}^{V_i} p_j(N-1)$ additions are needed to calculate the sample cumulants $\hat{\mathcal{C}}_{kx}(\mathbf{T})$. Additionally, for calculating the covariance matrix Σ, $\sum_{r=1}^{M}\sum_{z=1}^{M}\sum_{i=1}^{V_r}\sum_{j=1}^{V_z}\sum_{l_1=1}^{p_i}\sum_{l_2=1}^{q_j}[(\sum_{\substack{m_1=1\\ m_1\neq l_1}}^{p_i}\mu_{m_1} + \sum_{\substack{m_2=1\\ m_2\neq l_2}}^{q_j}\mu_{m_2})N + (\mu_{l_1}+\mu_{l_2})T^2 + 3T]$ multiplications and $\sum_{r=1}^{M}\sum_{z=1}^{M}\sum_{i=1}^{V_r}\sum_{j=1}^{V_z}\sum_{l_1=1}^{p_i}\sum_{l_2=1}^{q_j}((p_i+q_j-2)(N-1)+T(T+4))$ additions are needed. Notice that the computational complexity of the HCSR scheme is much higher, nearly M^2 fold, than that of the SCSR scheme. However, the HCSR scheme can provide a more accurate sensing and recognition performance than the SCSR scheme, which allows for a compromise between performance and computational complexity.

V. Discussions and Simulations

A. Discussions

We first analyze the theoretical statistical values for several non-Gaussian processes. By setting $\boldsymbol{\tau} = \mathbf{0}$, the theoretical values are calculated by averaging HOCs under the constraint of unit energy and noise-free case [36]. Table I gives the theoretical values of some typical non-Gaussian processes (e.g., digital modulated signals). Note that for the real-valued BPSK signal, the cumulants presented in Table I are all non-zeros. Moreover, it can be easily seen that with given k, the changes of l does not affect the kth-order cumulants for real-valued signals, which is consistent with the definition of cumulants Eq. (3). For all the complex-valued modulation schemes listed in Table I, the cumulants with $k=2, l=0$ and $k=4, l=1$ are zeros. Thus, the PU's signals and transmission power can not be recognized if we choose these parameters to perform the proposed spectrum sensing and power recognition schemes when the PUs' signal is complex-valued digital modulated signal. Therefore, we should choose proper k and l where the cumulants of the transmitted signal not only exist, but also are non-zeros. In the following simulations, we choose $k=4$ and $l=2$.

TABLE I
Some theoretical statistical cumulants values for various modulation schemes

Cumulant	$k=2, l=0$	$k=4, l=0$	$k=4, l=1$	$k=4, l=2$
BPSK	1	-2	-2	-2
QPSK	0	1	0	-1
8PSK	0	0	0	-1
16-QAM	0	-0.68	0	-0.68
64-QAM	0	-0.62	0	-0.62

Given k and l, the time lag $\boldsymbol{\tau}$ will also affect the cumulants of the random processes. As an intuitive understanding, when the time lags are far away from each other, then $x(n), x(n+\tau_1), \cdots, x(n+\tau_{k-1})$ will be independent, which will lead $c_{kx}(\boldsymbol{\tau})$ tend to zero. According to Eq. (3), moreover, cumulants of the complex-valued signals are complex values if the time lags are not equal to zeros. Fig. 3 shows the real part and imaginary part of fourth-order cumulants of various digital modulated signals, white Gaussian noise and colored Gaussian noise, by setting $\boldsymbol{\tau} = [0, 0, \tau], \tau = 0, \cdots, 20$. The sampling frequency adopted is 8 times of symbol rate. It can be seen that the fourth-order cumulants with small lags for non-Gaussian signals are not equal to zero, which is different from that of the Gaussian noise even when the noise is colored. Hence, we can employ fourth-order cumulants to extract non-Gaussian signal from Gaussian noise. On the other hand, with the increase of the time lag τ, fourth-order cumulants of digital modulated signals tend to zero. Thus, in the following simulations, we choose $\boldsymbol{\tau} = [0,0,0]$ to evaluate the proposed SCSR scheme and $\boldsymbol{\tau}_1 = [0,0,0]$, $\boldsymbol{\tau}_2 = [0,0,1]$ to evaluate the proposed HCSR scheme. The variances of cumulants estimation $\hat{c}_{k_1}(\boldsymbol{\tau}_1)$, $\hat{c}_{k_2}(\boldsymbol{\tau}_2)$ and the covariance between them can be estimated as:

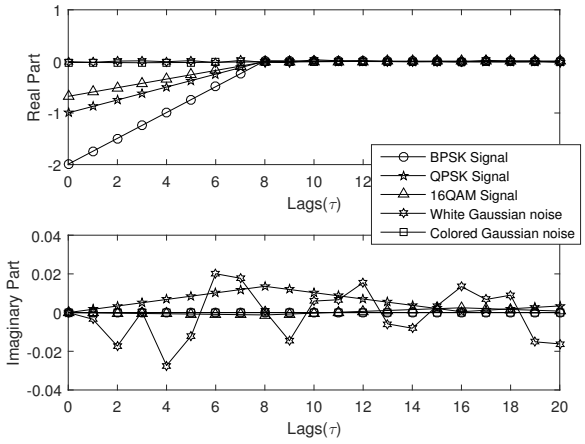

Fig. 3. Fourth-order cumulants of various random processes.

$$N\text{var}[\hat{c}_{k_1}(\boldsymbol{\tau}_1)] = \hat{Q}_{4,4}(\boldsymbol{\tau}_1,\boldsymbol{\tau}_1) - 12\hat{Q}_{4,2}(\boldsymbol{\tau}_1,0)\hat{m}_{2x}(0) + 36\hat{Q}_{2,2}(0,0)\hat{m}_{2x}(0)\hat{m}_{2x}(0) \quad (64)$$

$$N\text{var}[\hat{c}_{k_2}(\boldsymbol{\tau}_2)] = \hat{Q}_{4,4}(\boldsymbol{\tau}_2,\boldsymbol{\tau}_2) - 6\hat{Q}_{4,2}(\boldsymbol{\tau}_2,0)\hat{m}_{2x}(1) - 6\hat{Q}_{4,2}(\boldsymbol{\tau}_2,1)\hat{m}_{2x}(0) + 9\hat{Q}_{2,2}(0,0)\hat{m}_{2x}(1)\hat{m}_{2x}(1) + 18\hat{Q}_{2,2}(0,1)\hat{m}_{2x}(0)\hat{m}_{2x}(1) + 9\hat{Q}_{2,2}(1,1)\hat{m}_{2x}(0)\hat{m}_{2x}(0) \quad (65)$$

$$N\text{var}[\hat{c}_{k_1}(\boldsymbol{\tau}_1), \hat{c}_{k_2}(\boldsymbol{\tau}_2)] = \hat{Q}_{4,4}(\boldsymbol{\tau}_1,\boldsymbol{\tau}_2) - 6\hat{Q}_{4,2}(\boldsymbol{\tau}_2,0)\hat{m}_{2x}(0) - 3\hat{Q}_{4,2}(\boldsymbol{\tau}_1,0)\hat{m}_{2x}(1) - 3\hat{Q}_{4,2}(\boldsymbol{\tau}_1,1)\hat{m}_{2x}(0) + 18\hat{Q}_{2,2}(0,0)\hat{m}_{2x}(0)\hat{m}_{2x}(1) + 18\hat{Q}_{2,2}(0,1)\hat{m}_{2x}(0)\hat{m}_{2x}(0). \quad (66)$$

B. Simulation results

In this subsection, we present simulation results to evaluate the performance of the proposed SCSR and HCSR schemes. The PU's signal considered in the simulation is QPSK signal. The symbol rate and sampling frequency are set as above in Section V-A. We consider that PU has four transmission power levels, and the priori probabilities are set as $\Pr(\mathcal{H}_0) = 0.4$ and $\Pr(\mathcal{H}_i) = 0.15, i = 1,2,3,4$, respectively. The power levels

This article has been accepted for publication in a future issue of this journal, but has not been fully edited. Content may change prior to final publication. Citation information: DOI 10.1109/TWC.2017.2777488, IEEE Transactions on Wireless Communications

satisfy $P_1 : P_2 : P_3 : P_4 = 3 : 5 : 7 : 9$, and the average signal-to-noise ratio (SNR) is defined as $1/4\sum_{i=1}^{4} P_i/\sigma_w^2$. The noise $w(n)$ is assumed to be correlated with $a = -0.9$ and $\sigma_w^2 = 1$, that is $w(n) = 0.9w(n-1) + u(n)$, where $u(n)$ is the WGN with mean zero and unit variance. When there exists noise uncertainty, noise variance is no longer a constant, but an uniform distribution random variable in $[\sigma_w^2/\eta, \sigma_w^2\eta]$ where η is the noise uncertainty factor. Let $\rho = 10\log_{10}\eta$ represent the noise uncertainty factor in dB. All the simulation results are obtained and averaged from 10000 Monte Carlo runs.

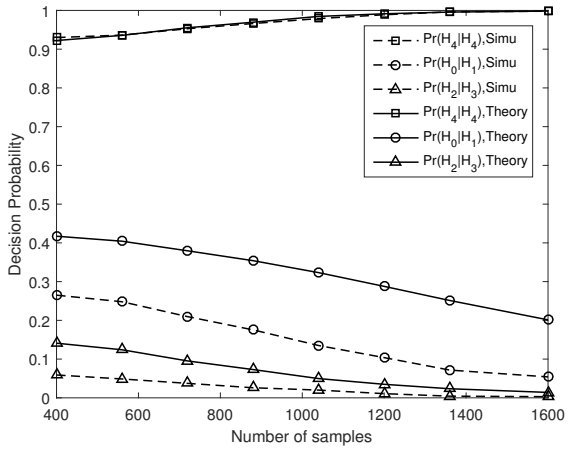

(a) Decision probability of SCSR scheme

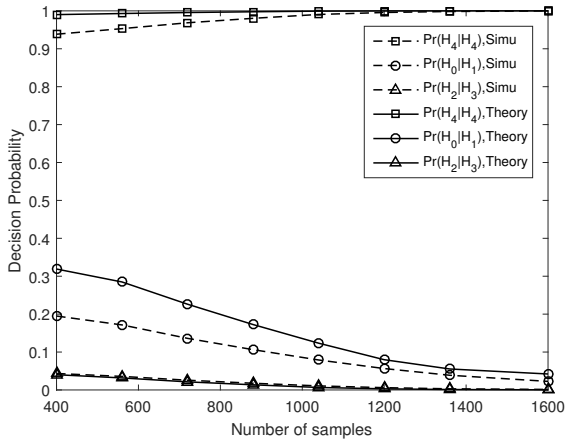

(b) Decision probability of HCSR scheme

Fig. 4. Theoretical analysis and numerical results for decision probability of SCSR and HCSR schemes.

Fig. 4 shows the theoretical analysis and numerical results for decision probability versus the number of samples with SNR$= -1$dB of SCSR and HCSR schemes, respectively. It can be seen that error detection probabilities for both SCSR and HCSR schemes are very low for any value of N. The theoretical curves are slightly higher than the simulated results. This is probably because the distributions obtained in (14) are asymptotic results rather than the exact values when the sample size is not large enough. Note that the gaps between the theoretical results and simulation results for both schemes reduce as the number of samples becomes larger, which proves the asymptotic properties of our proposed schemes.

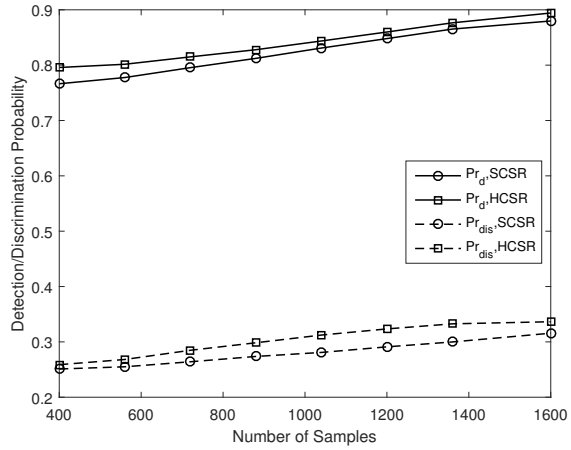

Fig. 5. The detection and discrimination probability versus number of samples of SCSR and HCSR schemes with SNR=-4dB.

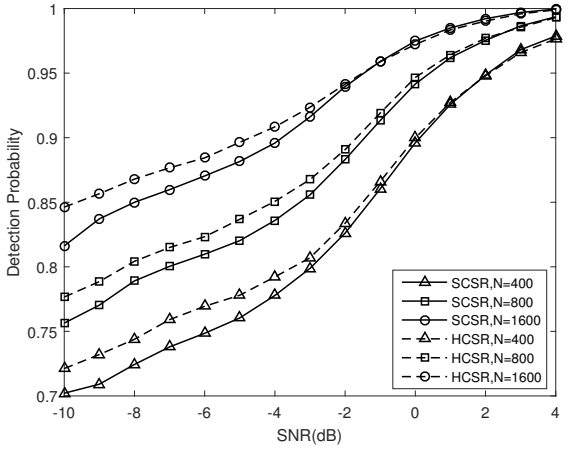

Fig. 6. The detection probability versus SNR of SCSR and HCSR schemes.

Fig. 5 shows the detection and discrimination probability versus number of samples for SCSR and HCSR schemes, respectively. It can be seen that both the detection and discrimination performance of HCSR scheme are much better than that of SCSR scheme, which means that HCSR scheme is more robust than SCSR scheme. This is because HCSR scheme exploits rich statistical information of the PU signal. Note that the detection probability is much higher than the discrimination probability for these two schemes. The reason is that even if PU is detected to be present, the SU might make mistakes in determining the PU's actual transmission power level. It can also be seen that the differences of both detection probability and discrimination probability between HCSR scheme and SCSR scheme diminish when the number of samples becomes greater. Nevertheless, both the detection and discrimination performance improve with the increase of N.

Fig. 6 shows the performance of detecting the "on/off" status of PU versus average SNR for both SCSR and HCSR schemes, respectively. The detection probability follows the definition in (18) and (51). From Fig. 6, it can be seen that the

This article has been accepted for publication in a future issue of this journal, but has not been fully edited. Content may change prior to final publication. Citation information: DOI 10.1109/TWC.2017.2777488, IEEE Transactions on Wireless Communications

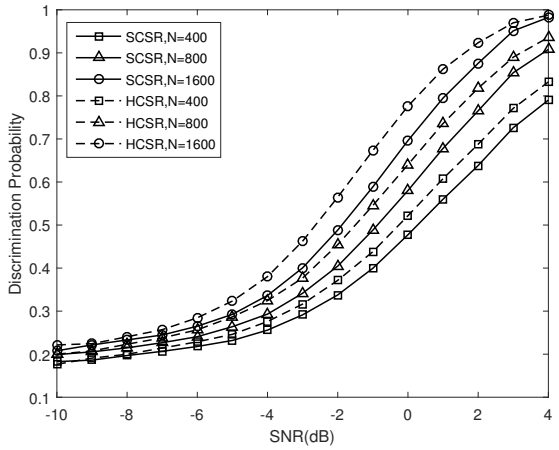

Fig. 7. The discrimination probability versus SNR of SCSR and HCSR schemes.

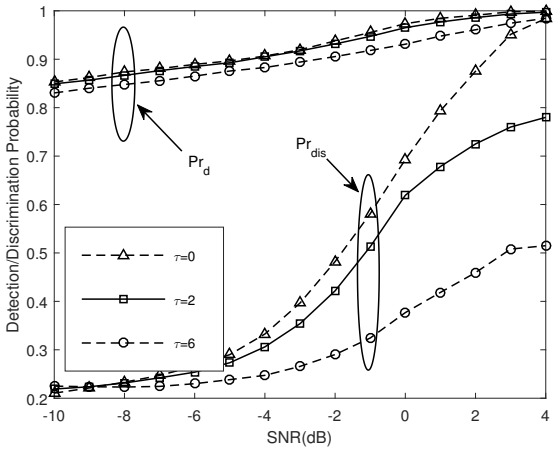

Fig. 8. The impact of time lag on the detection and discrimination probability of SCSR scheme.

detection performance improves dramatically with the increase of the received SNR in terms of both schemes. Moreover, it can also be seen that the gap between these two sensing schemes widens when the SNR becomes higher or the number of samples becomes greater. This implies that when the sensing conditions become better, the HCSR scheme is more robust than the SCSR scheme.

Fig. 7 shows the discrimination probability versus average SNR for SCSR and HCSR schemes, respectively. It can be seen that the discrimination probability of both schemes with 1600 samples is a little higher than that with 400 samples at low SNR condition. It implies that the increase of the sampling numbers can not attain the performance improvement effectively at low SNR condition. While the performance of the HCSR scheme with two different time lags is better than that of the SCSR scheme with only one time lag. This indicates that the increase of the number of adopted cumulants with different time lags can improve the discrimination capability of both proposed schemes. The amount of discrimination performance improvement from $N = 400$ to $N = 1600$ for each scheme is about 2dB. Additionally, it can also be seen that HCSR scheme outperforms SCSR scheme at any number of samples.

Fig. 8 shows the impact of time lag on the performance of SCSR scheme in terms of the detection probability and discrimination probability. In this simulation, we set the time lags $\boldsymbol{\tau} = [0, 0, \tau]$, where $\tau = 0, 2, 6$ respectively. The variance of cumulant estimate $\hat{c}_k(\boldsymbol{\tau})$ can be calculated by replacing 1 with τ in (65). It can be seen that both the detection probability and discrimination probability decrease with the increase of time lag τ. This is because that when the time lags are far from each other, the received samples will be independent with each other which leads the cumulants to diminish. This implies that the non-Gaussian information of the PU's transmitted signal can not be extracted effectively with a large time lag.

Fig. 9 shows the impact of noise uncertainty on the detection and discrimination performance of both SCSR and HCSR schemes. It is seen that the curves of either the detection probability or the discrimination probability with and without noise

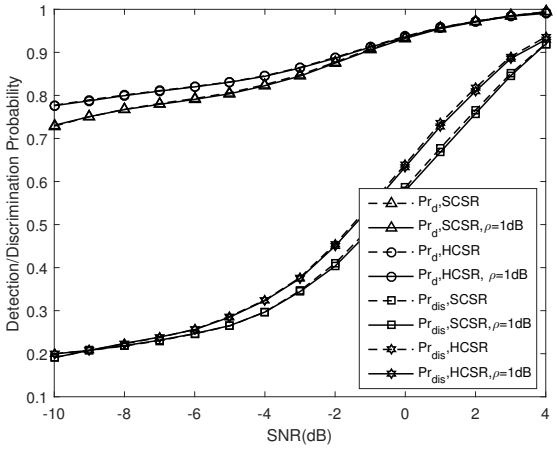

Fig. 9. The detection and discrimination probability versus SNR of SCSR and HCSR schemes with noise uncertainty.

uncertainty are almost overlapping for both SCSR scheme and HCSR scheme. It demonstrates that both the SCSR scheme and HCSR scheme are robust to the noise uncertainty. This is because that the derivation of the decision thresholds is not related to noise power. Moreover, we can see that HCSR scheme outperforms SCSR scheme in terms of both detection probability and discrimination probability which is consistent with the demonstration in Fig. 5.

VI. Conclusions

In this paper, we have proposed HOC based spectrum sensing and power recognition schemes for hybrid interweave-underlay spectrum access, considering PU has multiple transmission power levels and primary signals are non-Gaussian processes. Specifically, for a given HOC order and time lag, a SCSR scheme with low complexity has been proposed based on minimum Bayes risk criterion, which can shorten the spectrum sensing period and in turn prolong the data transmission period considerably. In addition, based on hybrid multiple HOCs, a HSCR scheme has been proposed by exploiting

This article has been accepted for publication in a future issue of this journal, but has not been fully edited. Content may change prior to final publication. Citation information: DOI 10.1109/TWC.2017.2777488, IEEE Transactions on Wireless Communications

the rich statistical information of the primary signal, which provides more accurate recognition performance to better protect PU from being harmfully interfered by SUs. We have discussed the power-mask effect and given new definitions of the performance metrics to analyze the sensing and recognition performance comprehensively. Moreover, the establishment of the decision regions for both SCSR and HCSR schemes do not depend on the noise power, and thus are robust to noise variance uncertainty. Finally, extensive simulations have been carried out to demonstrate that the proposed schemes can effectively recognize the transmission power level of PU when the primary signals are non-Gaussian process.

For the future work, we will investigate the decentralized collaborative spectrum sensing and power recognition in hybrid interweave-underlay CR networks, considering the spatial diversity of the multiple CR sensors.

APPENDIX A
DERIVATION OF THE MAP DECISION RULE

Denote $R_i = \{\hat{c}_{kx}(\boldsymbol{\tau}); \text{decide}\mathcal{H}_i\}$, and $R_i, i = 1, \cdots, L$ is the partition of the observation space. Then the Bayes risk (24) can be expanded as

$$\begin{aligned}\mathcal{R} &= \sum_{i=1}^{L}\sum_{j=1}^{L} K_{ij}\int_{R_i} p(\hat{c}_{kx}(\boldsymbol{\tau})|\mathcal{H}_j;\hat{\mathcal{H}}_{\text{on}})\text{Pr}(\mathcal{H}_j|\hat{\mathcal{H}}_{\text{on}})d\hat{c}_{kx}(\boldsymbol{\tau}) \\ &= \sum_{i=1}^{L}\int_{R_i}\sum_{j=1}^{L} K_{ij}p(\hat{c}_{kx}(\boldsymbol{\tau})|\mathcal{H}_j;\hat{\mathcal{H}}_{\text{on}})\text{Pr}(\mathcal{H}_j|\hat{\mathcal{H}}_{\text{on}})d\hat{c}_{kx}(\boldsymbol{\tau}) \\ &= \sum_{i=1}^{L}\int_{R_i}\sum_{j=1}^{L} K_{ij}\text{Pr}(\mathcal{H}_j|\hat{c}_{kx}(\boldsymbol{\tau});\hat{\mathcal{H}}_{\text{on}})p(\hat{c}_{kx}(\boldsymbol{\tau})|\hat{\mathcal{H}}_{\text{on}})d\hat{c}_{kx}(\boldsymbol{\tau}).\end{aligned} \tag{67}$$

Define $\mathcal{K}_i(\hat{c}_{kx}(\boldsymbol{\tau})) = \sum_{j=1}^{L} K_{ij}\text{Pr}(\mathcal{H}_j|\hat{c}_{kx}(\boldsymbol{\tau});\hat{\mathcal{H}}_{\text{on}})$ be the average cost of deciding $\mathcal{H}_i$ if $\hat{c}_{kx}(\boldsymbol{\tau})$ is observed. Then

$$\mathcal{R} = \sum_{i=1}^{L}\int_{R_i}\mathcal{K}_i(\hat{c}_{kx}(\boldsymbol{\tau}))p(\hat{c}_{kx}(\boldsymbol{\tau})|\hat{\mathcal{H}}_{\text{on}})d\hat{c}_{kx}(\boldsymbol{\tau}). \tag{68}$$

In order to minimize $\mathcal{R}$, we minimize $\mathcal{K}_i(\hat{c}_{kx}(\boldsymbol{\tau}))$, i.e., the decision rule can be conclude as

$$i^* = \arg\min_i \mathcal{K}_i(\hat{c}_{kx}(\boldsymbol{\tau})). \tag{69}$$

When the particular value of cost (26) is taken into consideration, the average cost can be expressed as

$$\begin{aligned}\mathcal{K}_i(\hat{c}_{kx}(\boldsymbol{\tau})) &= \sum_{\substack{j=1\\ j\neq i}}^{L}\text{Pr}(\mathcal{H}_j|\hat{c}_{kx}(\boldsymbol{\tau});\hat{\mathcal{H}}_{\text{on}}) \\ &= \sum_{j=1}^{L}\text{Pr}(\mathcal{H}_j|\hat{c}_{kx}(\boldsymbol{\tau});\hat{\mathcal{H}}_{\text{on}}) - \text{Pr}(\mathcal{H}_i|\hat{c}_{kx}(\boldsymbol{\tau});\hat{\mathcal{H}}_{\text{on}}).\end{aligned} \tag{70}$$

Since the first term is independent with i, $\mathcal{K}_i(\hat{c}_{kx}(\boldsymbol{\tau}))$ is minimized by maximizing $\text{Pr}(\mathcal{H}_i|\hat{c}_{kx}(\boldsymbol{\tau});\hat{\mathcal{H}}_{\text{on}})$. Thus, the decision rule turns into MAP criterion, i.e.,

$$i^* = \arg\max_i \text{Pr}(\mathcal{H}_i|\hat{c}_{kx}(\boldsymbol{\tau});\hat{\mathcal{H}}_{\text{on}}). \tag{71}$$

REFERENCES

[1] J. Mitola, "Cognitive radio for flexible mobile multimedia communications," *Mobile Networks and Applications*, vol. 6, no. 5, pp. 435–441, Sep. 2001.

[2] S. Haykin, "Cognitive radio: brain-empowered wireless communications," *IEEE J. Sel. Areas Commun.*, vol. 23, no. 2, pp. 201–220, Feb. 2005.

[3] N. Zhang, H. Liang, N. Cheng, Y. Tang, J. W. Mark, and X. Shen, "Dynamic spectrum access in multi-channel cognitive radio networks," *IEEE J. Sel. Areas Commun.*, vol. 32, no. 11, pp. 2053–2064, Nov. 2014.

[4] H. Xie, B. Wang, F. Gao, and S. Jin, "A full-space spectrum-sharing strategy for massive mimo cognitive radio systems," *IEEE J. Sel. Areas Commun.*, vol. 34, no. 10, pp. 2537–2549, Oct. 2016.

[5] A. Goldsmith, S. A. Jafar, I. Maric, and S. Srinivasa, "Breaking spectrum gridlock with cognitive radios: an information theoretic perspective," *Proceeding of the IEEE*, vol. 97, no. 5, pp. 894–914, 2009.

[6] Y. Xing, R. Chandramouli, S. Mangold, and S. S. N, "Dynamic spectrum access in open spectrum wireless networks," *IEEE J. Sel. Areas Commun.*, vol. 24, no. 3, pp. 626–637, Mar. 2006.

[7] L. B. Le and E. Hossain, "Resource allocation for spectrum underlay in cognitive radio networks," *IEEE Trans. Wireless Commun.*, vol. 7, no. 12, pp. 5306–5315, Dec. 2008.

[8] S. Sun, Y. Ju, and Y. Yamao, "Overlay cognitive radio OFDM system for 4G cellular networks," *IEEE Wireless Commun.*, vol. 20, no. 2, pp. 68–73, Apr. 2013.

[9] Y. Wang, P. Ren, F. Gao, and Z. Su, "A hybrid underlay/overlay transmission mode for cognitive radio networks with statistical quality-of-service provisioning," *IEEE Trans. Wireless Commun.*, vol. 13, no. 3, pp. 1482–1498, Mar. 2014.

[10] J. Zou, H. Xiong, D. Wang, and C. W. Chen, "Optimal power allocation for hybrid overlay/underlay spectrum sharing in multiband cognitive radio networks," *IEEE Trans. Veh. Technol.*, vol. 62, no. 4, pp. 1827–1837, May 2013.

[11] T. M. C. Chu, H. Phan, and H. J. Zepernick, "Hybrid interweave-underlay spectrum access for cognitive cooperative radio networks," *IEEE Trans. Commun.*, vol. 62, no. 7, pp. 2183–2197, Jul. 2014.

[12] M. Jazaie and A. R. Sharafat, "Downlink capacity and optimal power allocation in hybrid underlay-interweave secondary networks," *IEEE Trans. Wireless Commun.*, vol. 14, no. 5, pp. 2562–2570, May 2015.

[13] X. Kang, Y. C. Liang, H. K. Garg, and L. Zhang, "Sensing-based spectrum sharing in cognitive radio networks," *IEEE Trans. Veh. Technol.*, vol. 58, no. 8, pp. 4649–4654, Oct. 2009.

[14] N. Zhang, H. Zhou, K. Zheng, N. Cheng, J. W. Mark, and X. Shen, "Cooperative heterogeneous framework for spectrum harvesting in cognitive cellular network," *IEEE Commun. Mag.*, vol. 53, no. 5, pp. 60–67, May 2015.

[15] S. Chen, Y. Wang, W. Ma, and J. Chen, "Technical innovations promoting standard evolution: from TD-SCDMA to TD-LTE and beyond," *IEEE Wireless Commun.*, vol. 19, no. 1, pp. 60–66, Feb. 2012.

[16] H. Zhou, B. Liu, Y. Liu, N. Zhang, L. Gui, Y. Li, X. Shen, and Q. Yu, "A cooperative matching approach for resource management in dynamic spectrum access networks," *IEEE Trans. Wireless Commun.*, vol. 13, no. 2, pp. 1047–1057, Feb. 2014.

[17] J. Li, L. P. Qian, Y. J. A. Zhang, and L. Shen, "Global optimal rate control and scheduling for spectrum-sharing multi-hop networks," *IEEE Trans. Wireless Commun.*, vol. 15, no. 9, pp. 6462–6473, Sep. 2016.

[18] "Wireless LAN medium access control (MAC) and physical layer (PHY) specifications," IEEE Std 802.11, 1997.

[19] "User equipment (UE) radio transmission and reception," 3GPP, Tech. Rep. v.10.3.0, Release 10, June 2011.

[20] "Requirements for further advancements for evolved universal terrestrial radio access (E-UTRA) (LTE-Advanced)," 3GPP, Tech. Rep. v.10.0.0, Mar. 2011.

[21] J. Mitola III, "Software radio architecture: a mathematical perspective," *IEEE J. Sel. Areas Commun.*, vol. 17, no. 4, pp. 514–538, Apr. 1999.

[22] F. Gao, J. Li, T. Jiang, and W. Chen, "Sensing and recognition when primary user has multiple transmit power levels," *IEEE Trans. Signal Process.*, vol. 63, no. 10, pp. 2704–2717, May 2015.

[23] Z. Li, D. Wang, P. Qi, and B. Hao, "Maximum-eigenvalue-based sensing and power recognition for multiantenna cognitive radio system," *IEEE Trans. Veh. Technol.*, vol. 65, no. 10, pp. 8218–8229, Oct. 2016.

[24] M. J. Hinich and G. R. Wilson, "Detection of non-Gaussian signals in non-Gaussian noise using the bispectrum," *IEEE Trans. Acoust., Speech, and Signal Process.*, vol. 38, no. 7, pp. 1126–1131, July 1990.

[25] X. Liang, Z. Ding, and C. Xiao, "Optimized power allocation for packet retransmissions of non-Gaussian inputs through sequential AWGN channels," *IEEE Trans. Commun.*, vol. 60, no. 7, pp. 1889–1902, July 2012.
[26] R. Zhang, M. Wang, L. X. Cai, Z. Zheng, X. Shen, and L. L. Xie, "LTE-unlicensed: the future of spectrum aggregation for cellular networks," *IEEE Wireless Commun.*, vol. 22, no. 3, pp. 150–159, Jun. 2015.
[27] J. K. Tugnait, "On multiple antenna spectrum sensing under noise variance uncertainty and flat fading," *IEEE Trans. Signal Process*, vol. 60, no. 4, pp. 1823–1832, Apr. 2012.
[28] H. Fan, H. Fan, Q. Meng, Y. Zhang, and W. Feng, "Feature detection based on filter banks and higher order cumulants," in *2006 IEEE Int. Conf. on Inf. Acquisition*, Aug. 2006, pp. 562–566.
[29] J. K. Tugnait, "Detection of non-Gaussian signals using integrated polyspectrum," *IEEE Trans. Signal Process.*, vol. 42, no. 11, pp. 3137–3149, Nov. 1994.
[30] L. M. Garth and Y. Bresler, "A comparison of optimized higher order spectral detection techniques for non-Gaussian signals," *IEEE Trans. Signal Process.*, vol. 44, no. 5, pp. 1198–1213, May 1996.
[31] W. Han, C. Huang, J. Li, Z. Li, and S. Cui, "Correlation-based spectrum sensing with oversampling in cognitive radio," *IEEE J. Sel. Areas Commun.*, vol. 33, no. 5, pp. 788–802, May 2015.
[32] S. M. Kay, *Fundamentals of Statistical Signal Processing: Detection Theory*. Prentice Hall PTR, 1993.
[33] D. R. Brillinger, *Time series: data analysis and theory*, 2nd ed. Siam, 1981, vol. 36.
[34] A. V. Dandawate and G. B. Giannakis, "Asymptotic theory of mixed time averages and kth-order cyclic-moment and cumulant statistics," *IEEE Trans. Inf. Theory*, vol. 41, no. 1, pp. 216–232, Jan. 1995.
[35] ——, "Asymptotic properties and covariance expressions of kth-order sample moments and cumulants," in *Proc. 1993 Asilomar Conf. on Signals, Systems and Computers*, vol. 2, 1993, pp. 1186–1190.
[36] K. Hassan, I. Dayoub, W. Hamouda, C. N. Nzeza, and M. Berbineau, "Blind digital modulation identification for spatially-correlated mimo systems," *IEEE Trans. Wireless Commun.*, vol. 11, no. 2, pp. 683–693, Feb. 2012.